Journal of Sensor Science and Technology
Vol. 30, No. 6 (2021) pp. 369-375
http://dx.doi.org/10.46670/JSST.2021.30.6.369
pISSN 1225-5475/eISSN 2093-7563

Metal-organic frameworks-driven ZnO-functionalized carbon nanotube fiber for NO_2 sensor

Sungyoon Woo[1,*], Mingyeong Jo[1,*], Joon-Seok Lee[1], Seung-Ho Choi [1], Sungju Lee[2], Hyeon Su Jeong[2], and Seon-Jin Choi[1,+]

Abstract

In this study, heterogeneous ZnO/CNTF composites were developed to improve the NO_2-sensing response, facilitated by the self-heating property. Highly conductive and mechanically stable CNTFs were prepared by a wet-spinning process assisted by the liquid crystal (LC) behavior of CNTs. Metal-organic frameworks (MOFs) of ZIF-8 were precipitated on the surface of the CNTF (ZIF-8/CNTF) via one-pot synthesis in solution. The subsequent calcination process resulted in the formation of the ZnO/CNTF composites. The calcination temperatures were controlled at 400, 500, and 600 °C in an N_2 atmosphere to confirm the evolution of the microstructures and NO_2-sensing properties. Gas sensor characterization was performed at 100 °C by applying a DC voltage to induce Joule heating through the CNTF. The results revealed that the ZnO/CNTF composite after calcination at 500 °C (ZnO/CNTF-500) exhibited an improved response (R_{air}/R_{gas} = 1.086) toward 20 ppm NO_2 as compared to the pristine CNTF (R_{air}/R_{gas} = 1.063). Selective NO_2-sensing properties were demonstrated with negligible responses toward interfering gas species such as H_2S, NH_3, CO, and toluene. Our approach for the synthesis of MOF-driven ZnO/CNTF composites can provide a new strategy for the fabrication of wearable gas sensors integrated with textile materials.

Keywords : Metal-organic frameworks (MOFs), Carbon nanotube fiber (CNTF), Self-heating, Gas sensors, NO_2.

1. INTRODUCTION

Excessive inhalation of nitrogen dioxide (NO_2) at low concentrations (–1 ppm) can cause pulmonary disease and severe damage to the respiratory system, making NO_2 one of the most harmful gas species to human health [1]. The National Aeronautics and Space Administration (NASA) reported air pollution trends in major cities worldwide using high-resolution global satellite maps [2], revealing a significant increase in NO_2 concentration in 2014, particularly in East Asia, due to growing economies and the demand for fossil fuels. In view of this, new types of sensing platforms with potential flexible and wearable functions should be developed to realize real-time and rapid NO_2 detection.

Carbon nanotubes (CNTs) are attractive electrical transducer layers for chemical sensors [3-5]. However, the major limitations of pristine CNTs are their low response and selectivity owing to the stable surface chemical states for gas sensor applications [6]. Therefore, functionalization of surface additives and elevating the operating temperature are general approaches for improving the gas-sensing response and selectivity [7,8].

Metal-organic frameworks (MOFs) have been employed as functional materials in gas-sensing layers mainly because of their high porosity and large surface area [9-12]. For example, various carbon nanocomposites have been developed by the functionalization of MOFs on templates such as carbon fibers (CFs) [13], macro-porous carbon (MPC) [14,15], graphene oxide (GO) [16], CNTs [17-19], and fullerene [20]. In addition, MOF-driven nanostructures to form porous metal oxides have been demonstrated to facilitate the *p-n* junction effect for improved gas-sensing performance [21].

In this study, we propose porous polyhedral ZnO-functionalized carbon nanotube fibers (ZnO/CNTFs) for improved NO_2 sensors. To this end, carbonaceous fibers were first prepared via a wet-spinning process assisted by the liquid crystal behavior of CNTs

[1] Division of Materials Science and Engineering, Hanyang University, 222 Wangsimni-ro, Seongdong-gu, Seoul 04763, Republic of Korea
[2] Institute of Advanced Composite Materials, Korea Institute of Science and Technology (KIST), 92 Chudong-ro, Bongdong-eup, Wanju-gun, Jeonrabuk-do 55324, Republic of Korea
[+] Corresponding author: sjchoi27@hanyang.ac.kr
*These authors contributed equally to this work
(Received: Oct. 15, 2021, Revised : Nov. 19, 2021, Accepted : Nov. 26, 2021)

[5,22]. Liquid phase growth of ZIF-8 was performed by immersing CNTF in a precursor-containing solution, resulting in the homogeneous precipitation of ZIF-8 on the surface of CNTF (ZIF-8/CNTF). Subsequent heat treatment in an inert atmosphere was performed at elevated temperatures to form porous ZnO nanocubes on the CNTFs (ZnO/CNTF). The ZnO/CNTF exhibited an increased response toward NO_2 gas as compared with pristine CNTF, enabling the self-heating property of CNTFs to control the operating temperature. The MOF-driven ZnO/CNTF composite sensor can be integrated with textile materials for applications in wearable NO_2 sensors.

2. EXPERIMENTAL

2.1 Materials

Zinc nitrate hexahydrate ($Zn(NO_3)_2 \cdot 6H_2O$, 98%), 2-methylimidazole (2-MeIM, 99%), methanol (MeOH, 99.8%), and chlorosulfonic acid (CSA) were purchased from Sigma-Aldrich. Nitric acid (HNO_3), sulfuric acid (H_2SO_4), hydrogen peroxide (H_2O_2), acetone, and hydrochloric acid were purchased from Daejung Chemical & Materials (Korea). Single-walled CNT powders (Tuball™) were obtained from OCSiAl. All chemicals were used without further purification.

2.2 Synthesis of pristine CNTF

The CNT powders were purified using CSA to remove impurities. A concentrated CNT solution up to 4 wt% in CSA was prepared by dispersing the purified CNT powder. The wet-spinning process was performed to obtain continuous CNT fibers collected on a bobbin from a coagulation bath containing acetone. The collected CNT fibers were dried in a vacuum oven at 80 °C.

2.3 Synthesis of ZIF-8/CNTF and ZnO/CNTF

Individual solutions were prepared by dissolving 0.203 g of $Zn(NO_3)_2 \cdot 6H_2O$ and 0.108 g of 2-MeIM in 10 mL of MeOH. Then, these two solutions were mixed together with a pristine CNTF and stirred at 120 rpm for 40 min at room temperature. During stirring, the transparent solution turned white, indicating the growth of ZIF-8. ZIF-8/CNTF was obtained after drying at room temperature. To obtain the ZnO/CNTF, the as-synthesized ZIF-8/CNTF was calcined in an N_2 atmosphere at various temperatures (400, 500, and 600 °C) for 3 h with a ramping rate of 2 °C min^{-1}. After calcination, the samples were labeled as ZnO/CNTF-400, ZnO/CNTF-500, and ZnO/CNTF-600.

2.4 Gas sensing characteristic

The gas-sensing characteristics of the ZnO/CNTF samples (ZnO/CNTF-400, ZnO/CNTF-500, and ZnO/CNTF-600) were evaluated at a operating temperature of 100 °C. The operating temperature of the ZnO/CNTF was maintained at 100 °C by applying a DC voltage to induce self-heating of the CNTFs. After the stabilization step under exposure to baseline air for 12 h, NO_2 gas was injected for 10 min at a concentration in the range of 1–20 ppm. The gas response was calculated by monitoring the resistance changes, that is, R_{air}/R_{gas}, where R_{air} and R_{gas} are the resistances of the ZnO/CNTF sensors under exposure to baseline air and analyte gas, respectively, using a source measurement unit (Keithley 2400).

3. RESULTS AND DISCUSSIONS

The synthesis processes for ZnO/CNTF are schematically illustrated in Fig. 1. First, a one-pot synthesis method was conducted to form ZIF-8 on the pristine CNTF. Separate solutions of $Zn(NO_3)_2 \cdot 6H_2O$ and 2-MeIM in methanol were mixed together, and CNTF was immersed into the mixed solution to simultaneously precipitate ZIF-8 on the surface of the CNTF (Fig. 1(a), (b)). The CNTF possesses numerous functional groups on its surface, which provide nucleation sites for Zn^{2+} and 2-MeIM clusters, allowing homogeneous growth of ZIF-8 on the CNTF [23]. The one-pot synthesis is advantageous considering that ZIF-8 polyhedrons are tightly bonded to the CNTF chemically, leading to efficient transduction properties during the gas-sensing process compared to physical attachments. Subsequent heat treatment was performed at elevated temperatures to form porous ZnO nanocubes on CNTF (ZnO/CNTF) (Fig. 1(c)).

After the wet-spinning process, the pristine CNTF exhibited a continuous fibrous structure with high mechanical stability and flexibility (Fig. 2(a)). The microstructure and surface morphology were investigated via scanning electron microscopy (SEM) before and after the growth of ZIF-8. For the pristine CNTF, a rough surface morphology was observed with the aligned CNT bundles (Fig. 2(b), (c)). The CNTF was immersed in a solution containing Zn^{2+} and 2-MeIM to precipitate ZIF-8 on the surface, wherein the transparent solution turned into a white solution (Fig. 2(d)). The microstructure in which CNTFs homogeneously decorated with polyhedral ZIF-8 by one-pot synthesis was confirmed (Fig.

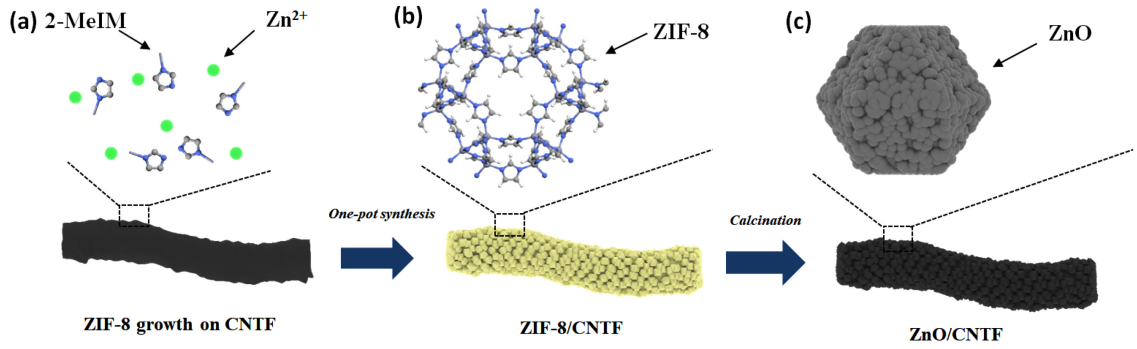

Fig. 1. Schematic illustrations of the synthesis of ZnO/CNTF: (a) Before and (b) after one-pot synthesis of ZIF-8 on CNTF. (c) ZnO/CNTF after calcination in N_2 atmosphere at elevated temperatures.

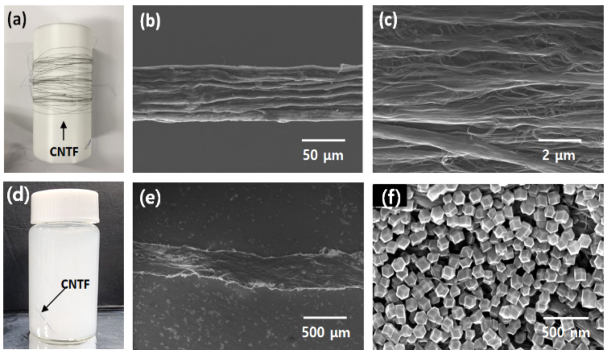

Fig. 2. (a) Photograph image of pristine CNT fiber. (b) SEM image of pristine CNT fiber and (c) its magnified SEM image. (d) One-pot synthesis of ZIF-8/CNTF in a mixture solution. (e) SEM image of ZIF-8/CNTF and (f) its magnified SEM image.

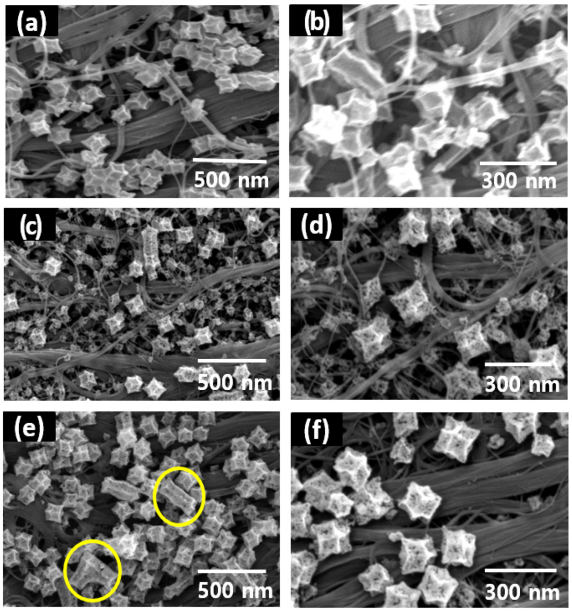

Fig. 3. SEM images of ZnO/CNTF calcined at (a)–(b) 400 °C (ZnO/CNTF-400), (c)–(d) 500 °C (ZnO/CNTF-500), and (e) –(f) 600 °C (ZnO/CNTF-600) in an N2 atmosphere for 3 h.

2(e),(f)).

Microstructural evolution during the calcination process at different temperatures (i.e., 400, 500, and 600 °C) in an N_2 atmosphere was investigated (Fig. 3). The ZnO/CNTF-400 exhibited a minor change in the shape and structure of ZIF-8 (Fig. 3(a), (b)). In addition, porous ZnO nanocubes were not obtained because of insufficient thermal energy at low temperatures [24]. On the other hand, ZnO/CNTF-500 (Fig. 3(c), (d)) and ZnO/CNTF-600 (Fig. 3(e), (f)) exhibited a highly porous structure after calcination of the ZIF-8/CNTF. The polyhedral ZIF-8 was converted into porous ZnO nanocubes after the calcination process, which was mainly achieved through the reaction between Zn from ZIF-8 and the oxygen functional groups on the CNTF. However, calcination at sufficiently high temperatures (i.e., 600 °C) induces agglomeration of ZnO nanocubes, as shown in the case of ZnO/CNTF-600 (yellow circles in Fig. 3(e)).

To improve the NO_2-sensing response, we utilized the self-heating effect by applying a voltage to the ZnO/CNTF, facilitating activated surface reaction kinetics. A suspended ZnO/CNTF sensor was fabricated on a glass substrate (2.5 cm × 1.0 cm) and a DC voltage was applied through the two probe tips (Fig. 4(a),(b)). An increased temperature of 100 °C was achieved for the ZnO/CNTF by Joule heating when the DC voltage was applied in the range of 2–3 V. For example, the heating temperature of the ZnO/CNTF-500 sensor was confirmed by an infrared camera, wherein a temperature of 100 °C was obtained under an applied voltage of 2.4 V (Fig. 4(c)). To investigate the heating property of ZnO/CNTF-500, voltage-dependent temperature changes were confirmed by slowly increasing the applied voltage (Fig. 4(d)-(f)). When voltage is applied, the temperature rises owing to the self-heating behavior of the CNTF [5]. In particular, ZnO/CNTF-500 exhibited step-like current-resistance transitions by increasing the voltages in the range of 0–2.4 V with a 0.4 V step. When 2.4 V

Table 1. Applied DC voltages to maintain the operating temperature at –100 °C for individual samples.

Sample	Temperature	Voltage
Pristine CNTF-400	102 °C	1.9 V
Pristine CNTF-500	100 °C	2.1 V
Pristine CNTF-600	102 °C	1.8 V
ZnO/CNTF-400	100 °C	3.0 V
ZnO/CNTF-500	102 °C	2.7 V
ZnO/CNTF-600	100 °C	3.0 V

was applied to the ZnO/CNTF-500, the maximum current and resistance of 64 mA and 38 Ω were obtained, respectively, resulting in an operating temperature of 100 °C. Reversible temperature transitions were observed as the sensor recovered the initial current by decreasing the voltage

The degree of self-heating according to the applied voltage varied with calcination temperatures of the ZnO/CNTFs. For this reason, different DC voltages were applied to the individual ZnO/CNTF and pristine CNTF samples, as summarized in Table 1, to equalize the operating temperature for NO_2 sensing as 100 °C. In the case of the ZnO/CNTF, slightly higher voltages (–3 V) should be applied to maintain 100 °C as compared to the pristine CNTF (–2 V), which was mainly attributed to the increased resistance of ZnO/CNTFs after the calcination process.

A comparative gas-sensing characterization was performed using pristine CNTF and ZnO/CNTF calcined at different temperatures toward NO_2 at an operating temperature of 100 °C (Fig. 5). All the sensors were stabilized under exposure to baseline air for 12 h to maintain a stable baseline resistance followed by the injection of NO_2 gas in the concentration range of 1–20 ppm. Both the pristine CNTF and ZnO/CNTF exhibited decreased resistance upon exposure to NO_2, indicating *p*-type-sensing properties. Dynamic response (R_{air}/R_{gas}) transitions were evaluated by comparing the CNTF and ZnO/CNTF at each calcination temperature. For the sensors with a calcination temperature of 400 °C, a decreased response of ZnO/CNTF-400 (R_{air}/R_{gas}=1.051) was obtained as compared to the response of the pristine CNTF-400 (R_{air}/R_{gas}=1.029) at 20 ppm NO_2 (Fig. 5(a)). The negligible improvement in the NO_2-sensing response of the ZnO/CNTF-400 sensor is mainly attributed to the insufficient oxidation of ZIF-8 at 400 °C, leading to a less porous structure of ZnO on the surface of the CNTF (Fig. 3(b)). On the other hand, a noticeable improvement in the responses was observed after calcination at 500 and 600 °C. For the ZnO/CNTF-500 sensor, the response was 1.086 at 20 ppm NO_2, which was slightly higher than that of the pristine CNTF-500 (R_{air}/R_{gas}=1.06) (Fig. 5(b)). Similarly, we obtained an enhanced response (R_{air}/R_{gas}=1.076) for ZnO/CNTF-600 at 20 ppm NO_2 as compared to the response (R_{air}/R_{gas}=1.047) of the pristine CNTF-600 (Fig. 5(c)). The increased NO_2-sensing responses after calcination at 500 and 600 °C were mainly attributed to the complete oxidation of ZIF-8 to form ZnO with high porosity (Fig. 3(d), (f)). However, the slightly reduced NO_2

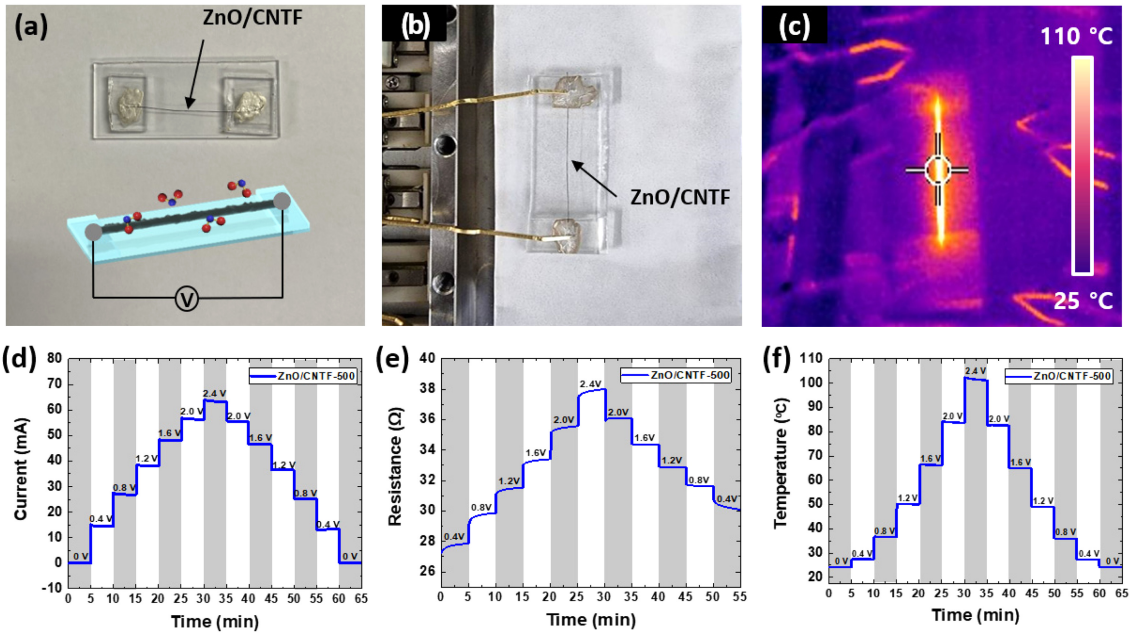

Fig. 4. (a) Camera image of ZnO/CNTF sensor for the detection of NO_2. (b) Camera image and (c) infrared camera image of ZnO/CNTF-500 sensor maintain operating temperatures at 100 °C under an applied voltage of 2.4 V. (d) Current, (e) resistance, and (f) temperature transitions of ZnO/CNTF-500 sensor under applied voltages in the range of 0–2.4 V with a 0.4 V step.

response of ZnO/CNTF-600 compared to that of ZnO/CNTF-500 was attributed to the agglomeration of ZnO nanocubes after excessive heat treatment at an elevated temperature, resulting in a decreased active surface area for the NO_2 reaction.

The improved NO_2 sensing mechanism of ZnO/CNTFs is discussed based on the resistance transitions and charge transfer behavior. Both CNTF and ZnO/CNTF exhibited decreased resistance upon exposure to NO_2. Because NO_2 is an oxidizing gas and has an electron-accepting nature, an increased hole concentration can be achieved in CNTF, resulting in *p*-type sensing. Considering that the pristine CNTF exhibited a NO_2-sensing response, there was a direct chemical interaction between NO_2 and CNTF. Specifically, surface-adsorbed nitrate (NO_3^-) can be formed on the surface of graphitic carbon based on the following chemical reaction [5]:

$$2NO_2\ (g) + O_2\ (g) + 2e^- \rightarrow 2NO_3^-\ (ads), \quad (1)$$

this chemical equation explains that the reason for decreasing resistance upon exposure to NO_2 is trapping of electrons, which increases the hole concentrations in the CNTF.

The improved NO_2-sensing response upon the functionalization of ZnO on CNTFs can be explained by electronic sensitization. ZnO is a well-known *n*-type semiconductor metal oxide, which can react with NO_2 via chemical adsorption, as shown below:

$$NO_2\ (g) + e^- \rightarrow NO_2^-\ (ads), \quad (2)$$

resulting in an electron trap on the ZnO surface. Hence, a decreased Fermi level of ZnO can be obtained while lowering the energy barrier between ZnO and CNTF, which results in facile electron transfer from CNTF to ZnO. This observation is consistent with the decreased resistance upon exposure to NO_2 as a result of the increased hole concentration in ZnO/CNTF [7]. Another reason for the improved NO_2 response can be attributed to the *p*-*n* junction formation between *n*-type ZnO and *p*-type CNTFs. The *p*-*n* junction forms a depletion layer, wherein the thickness of the depletion layer can be effectively modulated upon exposure to NO_2, leading to large resistance changes and a high response. In addition, the porous polyhedral structure of ZnO facilitates NO_2 penetration into the sensing layers, which induces efficient surface chemical reactions.

In terms of optimum sensing characteristics with respect to the calcination temperature, ZnO/CNTF-400 exhibited increased baseline resistance after heat treatment, which indicates the formation of ZnO by forming a *p*-*n* junction with CNTF.

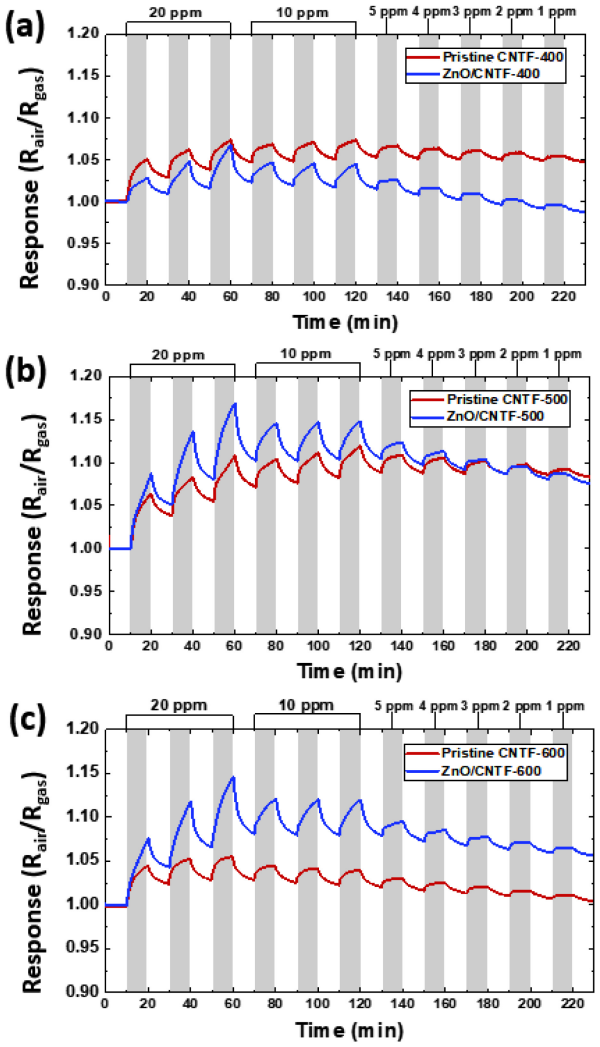

Fig. 5. Dynamic response transitions of pristine CNTF and ZnO/CNTF after calcination at (a) 400 °C, (b) 500 °C, and (c) 600 °C toward NO_2 gas in the concentration range of 1–20 ppm at the operating temperature of 100 °C.

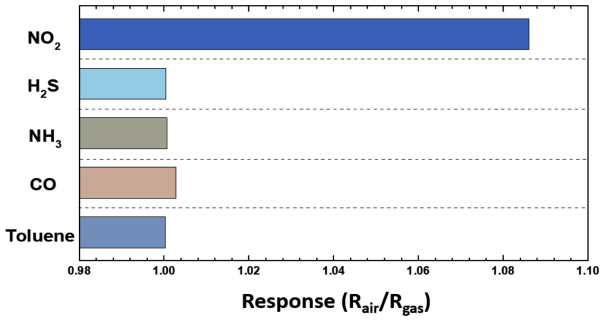

Fig. 6. Selective sensing property of ZnO/CNTF-500 sensor toward various gas species of 20 ppm at the operating temperature of 100 °C.

However, mesopores were not noticeably generated on the ZnO nanocubes because of insufficient calcination temperature,

resulting in a decreased NO_2 response. For ZnO/CNTF-500, we observed an increased baseline resistance, which is consistent with the formation of the *p-n* junction. In addition, highly porous ZnO nanocubes were uniformly decorated on the surface of the CNTF, leading to an improved NO_2 response. After calcination at 600 °C in N_2, the ZnO/CNTF-600 exhibited a decreased baseline resistance compared to the pristine CNTF-600. The decreased resistance is mainly attributed to the disappearance of the *p-n* junction. Indeed, excess heat treatment in an inert atmosphere can reduce ZnO, limiting the formation of the *p-n* junction [7]. Although porous ZnO nanocubes were formed on the surface of CNTF, the ZnO/CNTF-600 sensor exhibited a slightly decreased NO_2 response because of the inactive modulation of the depletion region formed by the *p-n* junction. Overall, the optimized calcination temperature was confirmed to be 500 °C considering the efficient charge transfer to ZnO, *p-n* junction formation, and decoration of porous ZnO nanocubes by forming a ZnO/CNTF composite.

The selective NO_2-sensing properties of ZnO/CNTF-500 were evaluated by exposure to various interfering gases, such as hydrogen sulfide (H_2S), ammonia (NH_3), carbon monoxide (CO), and toluene (C_7H_8) at 20 ppm (Fig. 6). The results confirmed that ZnO/CNTF-500 exhibited the highest response (R_{air}/R_{gas}) toward NO_2 (1.083) as compared to the response toward H_2S (1.0003), NH_3 (1.0007), CO (1.0028), and toluene (1.0004).

4. CONCLUSIONS

In this work, ZnO/CNTF composites were developed by homogeneous decoration of ZIF-8 on CNTF through one-pot synthesis and subsequent calcination in N_2 atmosphere. The microstructure of the ZnO/CNTF composites was investigated with respect to the calcination temperature. In particular, porous polyhedral ZnO nanocubes were deposited on the surface of CNTFs after calcination at 500 and 600 °C. In addition, the *p-n* junction was formed after calcination at 400 and 500 °C between the interfaces of *n*-type ZnO and *p*-type CNTF, which induces efficient modulation of the depletion layer, leading to improved NO_2-sensing properties. To activate the surface reaction kinetics, we utilized the self-heating property of CNTFs by applying a voltage to induce Joule heating. The operating temperature was maintained at 100 °C during gas-sensing characterization. As a result, an improved NO_2-sensing response (R_{air}/R_{gas}=1.086 at 20 ppm) was achieved with ZnO/CNTF-500. In addition, the ZnO/CNTF-500 exhibited high NO_2 selectivity with minor responses toward interfering gas species such as H_2S, NH_3, CO, and toluene. This study demonstrates a new approach for the synthesis of CNT-based sensing composites functionalized with MOF-driven ZnO nanocubes, which can be integrated with textile materials for wearable chemical sensors.

ACKNOWLEDGMENT

This work was supported by the National Research Foundation of Korea (NRF) grant funded by the Korean government (MSIT) (No. 2020R1C1C1010336). This work was also supported by the U.S. Army Combat Capabilities Development Command Soldier Center (DEVCOM SC) and International Technology Center Pacific (ITC-PAC) Global Research Project under contract FA520920P0130, and conducted at Hanyang University.

REFERENCES

[1] W. Huang, X. Zhuang, F. S. Melkonyan, B. Wang, L. Zeng, G. Wang, S. Han, M. J. Bedzyk, J. Yu, and T. J. Marks, "UV–Ozone interfacial modification in organic transistors for high-sensitivity NO_2 detection", *Adv. Mater.*, Vol. 29, No. 31, pp. 1701706(1)-1701706(11), 2017.

[2] S. Cole and E. Gray, *New NASA Satellite Maps Show Human Fingerprint on Global Air Quality*, NASA, RELEASE 15-233, 2015

[3] B. Yoon and S. J. Choi, "Selective acetate recognition and sensing using SWCNTs functionalized with croconamides", *Sens. Actuators B-Chem*, Vol. 346, pp. 130461(1)-130461(8), 2021.

[4] S. J. Choi, B. Yoon, J. D. Ray, A. Netchaev, L. C. Moores, and T. M. Swager, "Chemiresistors for the Real-Time Wireless Detection of Anions", *Adv. Func. Mater.*, Vol. 30, No. 7, pp. 1907087(1)-1907087(9), 2020.

[5] S. J. Choi, D. M. Lee, H. Yu, J. S. Jang, M. H. Kim, J. Y. Kang, H. S. Jeong, and I. D. Kim, "All-carbon fiber-based chemical sensor: Improved reversible NO_2 reaction kinetics", *Sens. Actuators B-Chem*, Vol. 290, pp. 293-301, 2019.

[6] T. Kawano, H. C. Chiamori, M. Suter, Q. Zhou, B. D. Sosnowchik, and L. Lin, "An electrothermal carbon nanotube gas sensor", *Nano Lett.*, Vol. 7, No. 12, pp. 3686-3690, 2007.

[7] J. Y. Kang, W. T. Koo, J. S. Jang, D. H. Kim, Y. J. Jeong, R. Kim, J. Ahn, S. J. Choi, and I. D. Kim, "2D layer assembly of Pt-ZnO nanoparticles on reduced graphene oxide for flexible NO_2 sensors", *Sens. Actuators B-Chem*, Vol. 331, pp. 129371(1)-129371(10), 2021.

[8] S. J. Choi, D. M. Lee, H. Yu, J. S. Jang, M. H. Kim, J. Y. Kang, H. S. Jeong, and I. D. Kim, "All-carbon fiber-based chemical sensor: Improved reversible NO_2 reaction kinetics", *Sens. Actuators B-Chem*, Vol. 290, pp. 293-301, 2019.

[9] H. Furukawa, N. Ko, Y. B. Go, N. Aratani, S. B. Choi, E. Choi, A. Ö. Yazaydin, R. Q. Snurr, M. O'Keeffe, and J. Kim, "Ultrahigh porosity in metal-organic frameworks", *Science*, Vol. 329, No. 5990, pp. 424-428, 2010.

[10] O. K. Farha, A. Ö. Yazaydın, I. Eryazici, C. D. Malliakas, B. G. Hauser, M. G. Kanatzidis, S. T. Nguyen, R. Q. Snurr, and J. T. Hupp, "De novo synthesis of a metal–organic framework material featuring ultrahigh surface area and gas storage capacities", *Nat. Chem.*, Vol. 2, No. 11, pp. 944-948, 2010.

[11] W. T. Koo, J. S. Jang, and I. D. Kim, "Metal-organic frameworks for chemiresistive sensors", *Chem*, Vol. 5, No. 8, pp. 1938-1963, 2019.

[12] D. J. Tranchemontagne, J. L. Mendoza-Cortés, M. O'Keeffe, and O. M. Yaghi, "Secondary building units, nets and bonding in the chemistry of metal-organic frameworks", *Chem. Soc. Rev.*, Vol. 38, No. 5, pp. 1257-1283, 2009.

[13] P. Pachfule, B. K. Balan, S. Kurungot, and R. Banerjee, "One-dimensional confinement of a nanosized metal organic framework in carbon nanofibers for improved gas adsorption", *Chem. Commun.*, Vol. 48, No. 14, pp. 2009-2011, 2012.

[14] Y. Zhang, X. Bo, C. Luhana, H. Wang, M. Li, and L. Guo, "Facile synthesis of a Cu-based MOF confined in macroporous carbon hybrid material with enhanced electrocatalytic ability", *Chem. Commun.*, Vol. 49, No. 61, pp. 6885-6887, 2013.

[15] Y. Zhang, X. Bo, A. Nsabimana, C. Han, M. Li, and L. Guo, "Electrocatalytically active cobalt-based metal–organic framework with incorporated macroporous carbon composite for electrochemical applications", *J. Mater. Chem. A*, Vol. 3, No. 2, pp. 732-738, 2015.

[16] C. Petit, and T. J. Bandosz, "Exploring the coordination chemistry of MOF–graphite oxide composites and their applications as adsorbents", *Dalton Trans.*, Vol. 41, No. 14, pp. 4027-4035, 2012.

[17] Z. Xiang, Z. Hu, D. Cao, W. Yang, J. Lu, B. Han, and W. Wang, "Metal–organic frameworks with incorporated carbon nanotubes: improving carbon dioxide and methane storage capacities by lithium doping", *Angew. Chem., Int. Ed.*, Vol. 50, No. 2, pp. 491-494, 2011.

[18] Y. Yang, L. Ge, V. Rudolph, and Z. Zhu, "In situ synthesis of zeolitic imidazolate frameworks/carbon nanotube composites with enhanced CO_2 adsorption", *Dalton Trans.*, Vol. 43, No. 19, pp. 7028-7036, 2014.

[19] R. Lin, L. Ge, S. Liu, V. Rudolph, and Z. Zhu, "Mixed-matrix membranes with metal–organic framework-decorated CNT fillers for efficient CO_2 separation", *ACS Appl. Mater. Interfaces*, Vol. 7, No. 27, pp. 14750-14757, 2015.

[20] A. W. Thornton, K. M. Nairn, J. M. Hill, A. J. Hill, and M. R. Hill, "Metal-organic frameworks impregnated with magnesium-decorated fullerenes for methane and hydrogen storage", *J. Am. Chem. Soc.*, Vol. 131, No. 30, pp. 10662-10669, 2009.

[21] W. T. Koo, S. J. Choi, S. J. Kim, J. S. Jang, H. L. Tuller, and I.-D. Kim, "Heterogeneous sensitization of metal–organic framework driven metal@metal oxide complex catalysts on an oxide nanofiber scaffold toward superior gas sensors", *J. Am. Chem. Soc.*, Vol. 138, No. 40, pp. 13431-13437, 2016.

[22] S. J. Choi, H. Yu, J. S. Jang, M. H. Kim, S. J. Kim, H. S. Jeong, and I. D. Kim, "Nitrogen-Doped Single Graphene Fiber with Platinum Water Dissociation Catalyst for Wearable Humidity Sensor", *Small*, Vol. 14, No. 13, pp. 1703934(1)-1703934(9), 2018.

[23] J. Wei, Y. Hu, Y. Liang, B. Kong, J. Zhang, J. Song, Q. Bao, G. P. Simon, S. P. Jiang, and H. Wang, "Nitrogen-doped nanoporous carbon/graphene nano-sandwiches: Synthesis and application for efficient oxygen reduction", *Adv. Func. Mater.*, Vol. 25, No. 36, pp. 5768-5777, 2015.

[24] P. Lin, L. Meng, Y. Huang, L. Liu, and D. Fan, "Simultaneously functionalization and reduction of graphene oxide containing isocyanate groups", *Appl. Surf. Sci.*, Vol. 324, pp. 784-790, 2015.